ISBN: 978-3-95450-227-1 ISSN: 2673-5490 doi:10.18429/JACoW-IPAC2022-WEPOMS029

MODELING OF THE OPTICAL STOCHASTIC COOLING AT THE IOTA STORAGE RING USING ELEGANT

A. J. Dick, P. Piot[1], Northern Illinois Center for Accelerator & Detector Development
Department of Physics, Northern Illinois University, DeKalb IL, USA
J. Jarvis, Fermi National Accelerator Laboratory, Batvia, IL, USA
[1]also at Argonne National Laboratory, Lemont, IL, USA

Abstract

In support of the Optical Stochastic Cooling (OSC) experiment at IOTA, we implemented a high-fidelity model of OSC in the ELEGANT beam-dynamics program. The introduced element is applicable to any OSC configurations and models the main features of OSC including (*i*) the longitudinal time of flight OSC, (*ii*) the effects between the transverse motion of particles in the beam and the transverse distribution of undulator radiation, and (*iii*) the incoherent contributions of neighboring particles. Together these produce a highly accurate model of OSC and were benchmarked using the results from the IOTA OSC experiment.

BACKGROUND

Stochastic Cooling is a beam cooling technique which uses electromagnetic radiation produced by a beam in a storage ring at a specific location (the pickup) to provide a corrective kick to the beam at a point downstream (the kicker). Radiation with bandwidth $\delta\omega$ carries information on temporal slices with duration $\tau \sim 1/\delta\omega$ so that the kick corrects the mean properties of these slices. When applied over millions of turns, this corrective kick reduces the momentum spread of the stored beam. The ability for this method to correct a single particle is limited by the number of other particles in the sample slice which act as random fluctuations on the single-particle cooling force. Optical Stochastic Cooling (OSC) extends this principle to the optical range using undulator magnets for the pickup and kicker [1]. The use of optical radiation increases the bandwidth of the signal compared to conventional microwave stochastic cooling. This increased bandwidth ultimately results in a faster cooling.

An exact simulation of OSC would require use of a finite difference time-domain software to calculate the production and interaction of the undulator radiation with the beam. This would be too computationally prohibitive considering the stochastic nature and the number of turns required to cool the beam. Instead we have implemented a semi-analytical model of OSC in ELEGANT, a particle tracking software used to simulate storage rings and beam lines [2]. The model includes three main components: (i) the so-called transit-time OSC, (ii) effects of transverse beam size, and (iii) incoherent contributions of other particles in the sample slice.

MODEL

The model we have implemented considers two planar undulator elements as the pickup and kicker elements. The kicker element changes each particle's momentum depending on (*i*) the arrival time of each particle relative to its own radiation, (*ii*) the transverse motion of each particle from the pickup to kicker, and (*iii*) any incoherent kicks due to nearby particles (as determined by the system bandwidth).

Transit-Time OSC

Transit-time OSC introduces an energy-dependent delay between the pickup and kicker using a particle bypass [3]. Particles which deviate from the reference energy arrive in the kicker out of phase with their radiation produced at the pickup and receive a kick proportional to this delay. Considering only the longitudinal motion, the momentum kick experienced by the i-th nacroparticle is

$$\delta p_i/p = -\kappa \sin\left[\omega(t_i - t_0) + \psi\right], \tag{1}$$

where κ is the maximum kick strength, $\omega = 2\pi/\lambda$ (where λ is the fundamental wavelength of the undulator radiation) is the angular frequency, and ψ is a phase offset which accounts for optical delay. The difference $t_i - t_0$ is the difference between the time-of-flight of the i-th macroparticle and the mean time-of-flight of the bunch. Both κ and ψ are user-controlled parameters which can be modified on a turn-by-turn basis.

Transverse Effects

Undulator radiation produced in the pickup is emitted in a cone with $\theta = 1/\gamma$ and is imaged to the same point in the kicker undulator. A particle may arrive off-axis relative to its own radiation due to transverse motion between the pickup and kicker especially for larger transverse beam sizes. The far-field radiation of a single particle at the focusing lens is,

$$E_x(\rho, \phi) = \frac{\theta\left[J_0(\xi) + (\gamma\theta)^2 \cos(2\phi) J_2(\xi)\right]}{(1 + (\gamma\theta)^2)^4}, \tag{2}$$

where $\xi \equiv \rho k_0 \theta/(1 + (\gamma\theta)^2)$, J_0 and J_2 are Bessel functions of the first kind of $n = 0, 2$, $k_0 = 2\pi/\lambda$ is the wave number, γ is the Lorentz factor, and θ is the angle of the emitted radiation. The total field is found by integrating Eq. 2 from 0 to θ_m, the angular acceptance of the lens. The effects of transverse displacement at the kicker can be modeled by taking the strength of the off-axis field relative to the on-axis field $E_x(\Delta x, \Delta y)/E_x(0,0)$ and multiplying it by the nominal kick strength. Eq. 1 then becomes,

$$\delta p_i/p = -\kappa \sin\left[\omega(t_i - t_0) + \psi\right] \times \frac{E_x(\Delta x, \Delta y)}{E_x(0,0)} \tag{3}$$

Content from this work may be used under the terms of the CC BY 4.0 licence (© 2022). Any distribution of this work must maintain attribution to the author(s), title of the work, publisher, and DOI

ISBN: 978-3-95450-227-1 ISSN: 2673-5490 doi:10.18429/JACoW-IPAC2022-WEPOMS029

Content from this work may be used under the terms of the CC BY 4.0 licence (© 2022). Any distribution of this work must maintain attribution to the author(s), title of the work, publisher, and DOI

where the quantities Δx and Δy are the difference in each particle's transverse position defined as $\Delta x = x_k - \mathcal{M}x_p$ (with $\mathcal{M}$ is the magnification of the optical line).

Incoherent Effects

So far the model neglects the effects due to other particles in the sample slice. This choice is justified for the case of the passive IOTA experiment as the charge is relatively low and the bunch length is relatively long contributing to sparsely populated sample slices. However, at high charge and low longitudinal spread, the incoherent contributions become significant. Any particle $N_u\lambda$ before or after the ith particle in the kicker will contribute to the kick the ith particle experiences in the kicker. This is implemented in our model by scanning over the array of particles, sorted by longitudinal position, and applying a kick to the ith particle for any particle in the sample slice. The interaction is modeled as,

$$\delta p_i/p = -\kappa(\widetilde{\psi}_{i,j}) \sin[\omega(t_i - t_0) + \psi + \widetilde{\psi}_{i,j}] \qquad (4)$$

which is the same as Eq. 1 with the phase term $\widetilde{\psi}_{i,j}$ representing the relative phase between the ith and jth particle. Additionally, the strength of the incoherent kick falls off linearly with the distance between the two until $\Delta z = N_u\lambda$.

BENCHMARKING

OSC was demonstrated at Fermilab's IOTA storage ring [4, 5] and data collected during the passive-OSC experiment were instrumental in benchmarking the computational model [6]. The primary metrics on which we evaluated the model were (*i*) the cooling rates of various lattice configurations and (*ii*) the equilibrium bunch length and transverse beam sizes. A complete lattice of the IOTA ring was simulated in ELEGANT using magnet settings from the experiment. The basic lattice cools the beam only in the longitudinal plane. However, this cooling force can be shared with the horizontal plane powering quadrupole magnet located in the particle bypass (with significant horizontal dispersion). The cooling force can further be shared with the vertical plane by placing a skew-quadrupole magnet in the lattice to couple the x and y planes. These two quadrupole magnets were the only lattice elements that were changed during the benchmarking process to investigate the cooling dynamics in all three coupling modes.

Before simulating the OSC elements, we produced a lattice file of the IOTA ring in ELEGANT to match experimental observations of the rf-system, synchrotron damping, and gas scattering. This lattice was taken directly from the IOTA experiment and Table 1 shows a comparison between some key parameters.

Synchrotron Damping Rates

The rate of synchrotron radiation (SR) damping was also measured in ELEGANT simulations before implementing the OSC elements. This confirmed both the lattice configuration and cooling rate analysis worked as expected. The SR damping rates, listed in Table 2, were measured to be $\lambda_x = 1.0\ s^{-1}$, $\lambda_y = 1.0\ s^{-1}$, and $\lambda_s = 1.9\ s^{-1}$ which agree well with the theoretical values of $\lambda_x = \lambda_y = 1.0\ s^{-1}$ and $\lambda_s = 2.0\ s^{-1}$.

Table 1: Comparison of Basic Lattice Parameters Between IOTA Experiment and ELEGANT Simulations

Parameter	IOTA Design		ELEGANT	
E loss per turn, eV	13.2		13.82	
Betatron tune ν_x/ν_y	5.42	2.42	5.42	2.42
Chromaticity ξ_x/ξ_y	-10.2	-8.1	-13.2	-6.15
Mom. Compaction	0.00493		0.004905	
Synchrotron Freq. (Hz)	426.5		426.1	

Table 2: Simulated Damping Rates for Synchrotron Radiation (SR) and Various Configurations of OSC

Coupling Mode	λ_s (s^{-1})	λ_x (s^{-1})	λ_y (s^{-1})
SR	1.0	2.0	1.9
s (1D)	27.7	2.0	-
s/x ((2D)	20.0	6.5	-
$s/x/y$ (3D)	19.7	4.5	3.7

OSC Cooling Rates

The cooling rates and equilibrium values were measured for all three coupling modes (s, s/x, s/x/y). Figure 1 shows each simulation beginning with a bunch near SR damping equilibrium which comprises 256 nacroparticles. In the IOTA experiment, residual gas effects increased the transverse SR-determined equilibrium by a factor of 2. The impact of residual gas was modeled by the SCATTER element which applies a Gaussian-distributed kick at each turn. The kick strength was altered until the simulation matched the experimentally-measured equilibrium emittances. The cooling rate can be measured directly by fitting an exponential decay function $\varepsilon(t) = (\varepsilon_0 - \varepsilon_{eq})e^{-rt} + \varepsilon_{eq}$ to the emittance curve.

The cooling force is shared between the degrees of freedom in the various coupling modes as depicted in Fig. 2. In the longitudinal only (1D) configuration, the horizontal emittance remains unaffected at the SR equilibrium point whereas in the s-x (2D) coupling configuration, the horizontal emittance decreases while the bunch length is cooled at a lower pace than for the 1D configuration.

OSC Heating & Higher-Order Attractors

Additionally, the OSC scheme can be used to heat the beam by tuning the optical delay so that the beam and radiation arrive π out of phase. In the case of longitudinal-only (1D) OSC heating, each particle is pushed toward a fixed point in high amplitude synchrotron motion; see Fig. 3. The point, determined by the radiation wavelength is approximately 200 mm.

The cooling range of OSC is limited by the wavelength of the undulator radiation. Particles with high synchrotron amplitudes will find themselves, on average, beyond the first

ISBN: 978-3-95450-227-1 ISSN: 2673-5490 doi:10.18429/JACoW-IPAC2022-WEPOMS029

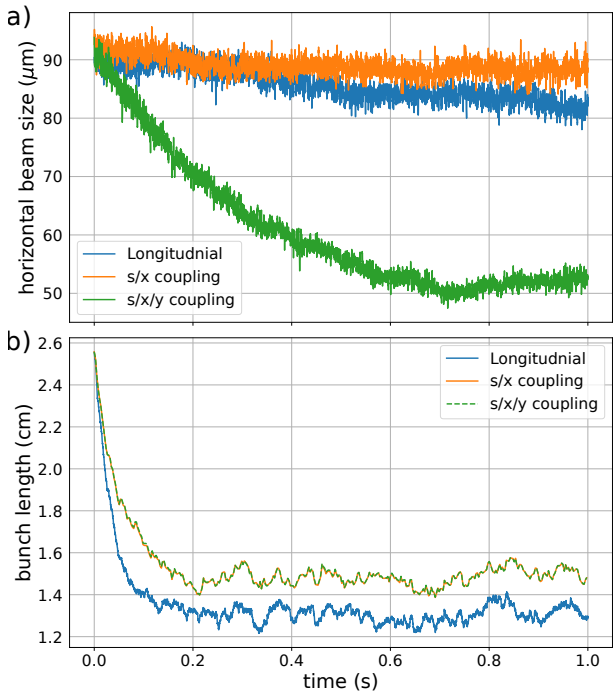

Figure 1: Horizontal emittance (a) and r.m.s. bunch length (b) of a beam undergoing OSC in the longitudinal-only (blue trace) and $s-x$ coupling (orange trace) configurations.

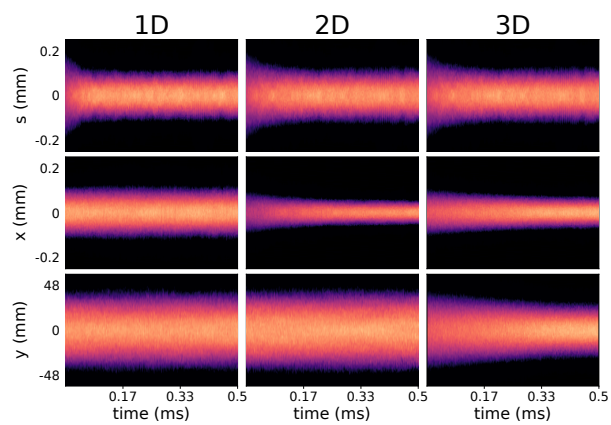

Figure 2: Waterfall plot of the longitudinal (top), horizontal (middle), and vertical (bottom) beam distributions for each of the three coupling modes.

order cooling effects and will be pushed toward higher-order attractors. This behavior can also be seen in the computational model by heating then cooling a beam. We introduce a beam near equilibrium then sweep the delay phase slowly alternating between heating and cooling, as shown in Fig. 4. As a result the bunch length alternatively lengthen (heating) and shorten (cooling) as the optical delay phase is varied. In the cooling regions, the beam consists of a bright core with low synchrotron amplitude and low energy spread. However, a small number of particles find themselves trapped in the first cooling attractor; see Fig. 4 for times $t \in [16, 28]$ ms.

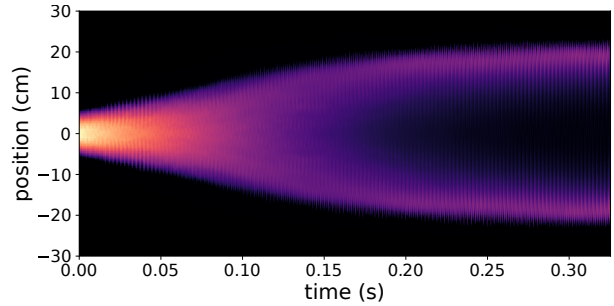

Figure 3: Waterfall plot of the longitudinal beam distribution showcasing the dynamics associated with the heating mode.

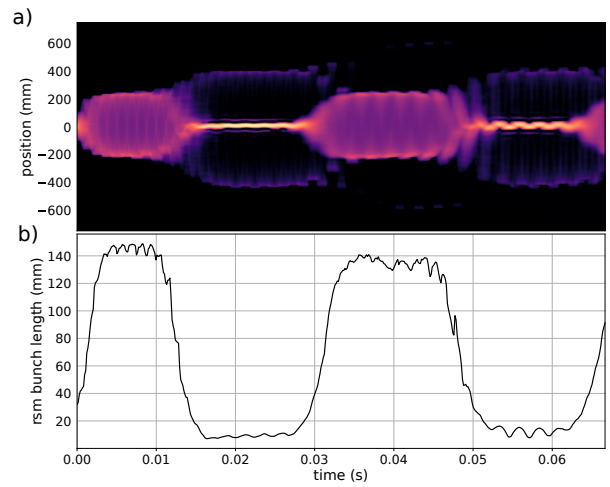

Figure 4: Waterfall plot of the longitudinal distribution (top) and resulting bunch length (bottom) as the optical delay between the radiation field and the beam in the kicker undulator is varied from $\pi/2$ to $5\pi/2$ showing the heating and cooling modes as well as higher order attractors.

CONCLUSION

We have developed a high-fidelity computational model of OSC in ELEGANT which correctly simulates the cooling and heating dynamics experimentally observed at IOTA. The model will provide guidance to design the planned active-OSC experiment, in which the undulator radiation will be amplified before being reintroduced in the kicker, and for understanding possible applications of OSC beyond beam cooling and preservation. Likewise, the developed tool will support the exploration of beam manipulation based on the interaction of the beam with its own fields [7].

ACKNOWLEDGEMENTS

Work supported by U.S. Department of Energy under award No. DE-SC0013761 with Northern Illinois University and by the U.S. National Science Foundation under award PHY-1549132, the Center for Bright Beams. The work of AD is partially supported by the DOE Office of Science Graduate Student Research (SCGSR) Program. Fermilab is managed by the Fermi Research Alliance, LLC for the DOE under contract number DE-AC02-07CH11359.

Content from this work may be used under the terms of the CC BY 4.0 licence (© 2022). Any distribution of this work must maintain attribution to the author(s), title of the work, publisher, and DOI

ISBN: 978-3-95450-227-1 ISSN: 2673-5490 doi:10.18429/JACoW-IPAC2022-WEPOMS029

Content from this work may be used under the terms of the CC BY 4.0 licence (© 2022). Any distribution of this work must maintain attribution to the author(s), title of the work, publisher, and DOI

REFERENCES

[1] A. A. Mikhailichenko and M. S. Zolotorev, "Optical stochastic cooling," *Phys. Rev. Lett.*, vol. 71, pp. 4146–4149, 1993, doi:10.1103/PhysRevLett.71.4146

[2] M. Borland, "ELEGANT: A Flexible SDDS-Compliant Code for Accelerator Simulation," in *6th International Computational Accelerator Physics Conference (ICAP 2000)*, 2000, doi:10.2172/761286

[3] M. S. Zolotorev and A. A. Zholents, "Transit-time method of optical stochastic cooling," *Phys. Rev. E*, vol. 50, pp. 3087–3091, 4 1994, doi:10.1103/PhysRevE.50.3087

[4] S. Antipov *et al.*, "IOTA (Integrable Optics Test Accelerator): Facility and experimental beam physics program," *J. Instrum.*, vol. 12, no. 03, T03002–T03002, 2017, doi:10.1088/1748-0221/12/03/t03002

[5] V. Lebedev, J. Jarvis, H. Piekarz, A. Romanov, J. Ruan, and M. Andorf, "The design of optical stochastic cooling for IOTA," *J. Instrum.*, vol. 16, no. 05, T05002, 2021, doi:10.1088/1748-0221/16/05/t05002

[6] J. Jarvis *et al.*, "First experimental demonstration of optical stochastic cooling," FERMILAB-PUB-22-093-AD, 2022, doi:10.48550/arXiv.2203.08899

[7] A. J. Dick and P. Piot, "Electron beam shaping techniques using optical stochastic cooling," presented at IPAC'22, Bangkok, Thailand, Jun. 2022, paper WEPOMS028, this conference.